Densification and microstructure of Si_3N_4-TiN ceramic composites

T. S. Ferreira[1*], F. M. S. Carvalho[2], C. C. Guedes-Silva[1]

[1]Instituto de Pesquisas Energéticas e Nucleares, Comissão Nacional de Energia Nuclear, Av. Prof. Lineu Prestes 2242, 05508-000, S. Paulo, SP, Brazil

[2]Universidade de São Paulo, Instituto de Geociências, 05508-080, S. Paulo, SP, Brazil

Abstract

Silicon nitride is a ceramic material widely used in various structural applications at high temperatures owing to its excellent combination of mechanical and thermal properties. To increase the application of Si_3N_4, many researches have been developed to improve its fracture toughness and processing conditions. In this study, the sintering and microstructure of Si_3N_4-TiN composites, containing Al_2O_3 and Y_2O_3 as sintering aids, were studied. Samples were obtained by the conventional method of mixing powders and sintered at 1750 ºC/1 h and 1815 ºC/1 h under nitrogen atmosphere. Density values of the samples were determined by the Archimedes method, reaching values between 96.9% and 98.0% of theoretical density, with a porosity of less than 0.5%. The sintered samples were analyzed by X-ray powder diffraction and scanning electron microscopy. The results showed the materials reached high fracture toughness, low hardness and a microstructure with TiN grains dispersed in a β-Si_3N_4 matrix containing an amorphous intergranular phase.

Keywords: silicon nitride, titanium nitride, sintering, microstructure.

INTRODUCTION

Silicon nitride (Si_3N_4) is one of the ceramic materials with varied applications due to its excellent thermo-mechanical properties, such as high hardness, strength, and resistance to thermal shock. These properties, combined with its low density, have allowed it to be extensively studied and used since the 1960s as a structural material in the manufacture of engine parts, bearings and turbines, grinding media, refractories, filters, magnetic sensors and thermocouples [1, 2]. In addition, in recent decades, the biocompatibility of this material has been verified, promoting its application in dental implants and orthopedic prostheses [3]. Silicon nitride presents two polymorphic states: α and β. Both phases are hexagonal, but the α-Si_3N_4 phase presents trigonal symmetry in a sequence of ABCD crystalline planes, while the β-Si_3N_4 phase has a hexagonal symmetry in an ABAB sequence. The different crystalline structures generate changes in grain morphology - equiaxial in the α phase and elongated in the β-phase. The elongated grains of the β-Si_3N_4 act as a reinforcement in the microstructure of the material, promoting the energy absorption by the crack deflection and increasing the material fracture toughness (K_{IC}), usually followed by reduction of the hardness and Young's modulus [4, 5].

Some factors limit the application field of silicon nitride, such as the high cost of the raw material and the complex processing. Its fracture toughness is also a property to be improved, being the subject of numerous researches [1, 4, 6]. In order to obtain ceramic bodies with high densities and excellent mechanical properties, it is necessary to use starting powders with reduced particle sizes and to submit them to a suitable sintering process [6, 7]. As silicon nitride is a covalent ceramic, the low diffusion coefficient difficult its sintering by means of solid-state diffusion mechanisms, making it difficult to obtain ceramic bodies with high densities. Since a silica layer is always present on the silicon nitride powder surface, one way to obtain dense components of silicon nitride is using additives to react with this silica layer in order to promote the liquid phase sintering [8]. In the liquid phase sintering process, particle rearrangement, liquid phase formation and the dissolution of the α-Si_3N_4 phase in the liquid phase should occur until the saturation. Subsequently, the α-Si_3N_4 phase reprecipitates as the β-Si_3N_4 phase, thermodynamically stable. Coalescence occurs in the last stage of the sintering characterized by the growth of β-Si_3N_4 grains which must be controlled to preserve the good mechanical properties of the final material [9, 10]. After cooling, the liquid phase remains in the grain boundaries of the material as secondary crystalline phases and/or as a glassy phase. The characteristics of the secondary intergranular phase allow controlling the material's microstructure according to the type and amount of additives besides the sintering technique used [9].

Researches [11] have shown that the various combinations of additives and sintering techniques still produce silicon nitride ceramics with low fracture toughness which is a barrier for several applications. To improve the mechanical properties, mainly the fracture toughness, and extend the potential of this ceramic in structural applications, the development of silicon nitride composites has been explored. The composites have a second phase as a reinforcement which may be in particle, fiber or whisker shape. For the reinforcement to play its role efficiently, some characteristics such as chemical compatibility and similar coefficients of

**tsferreira@ipen.br*

https://orcid.org/0000-0001-5130-6024

thermal expansion should be considered [11]. Among the silicon nitride composites, the most important are Si_3N_4-SiC [12, 13], Si_3N_4-ZrB_2, Si_3N_4-BN and Si_3N_4-TiN [14-23]. The Si_3N_4-TiN composite is used in structural and studied for biomedical applications due to its high mechanical strength, low density, and good electrical properties. The presence of dispersed TiN particles in the Si_3N_4 matrix makes it possible to obtain materials with high fracture toughness and flexural strength, high hardness, high chemical and wear resistance and high melt temperature [14, 15]. As the TiN second phase presents considerable electrical conductivity, a reduction occurs in the electrical resistivity of the material, allowing its machining by electric discharge [16-22]. In the present study, we investigated the effect of different contents of TiN in densification and microstructure of Si_3N_4-TiN composites also using Al_2O_3 and Y_2O_3 as sintering aids. The study was performed by the conventional process of pressureless sintering at 1750 ºC/1 h and 1815 ºC/1 h.

EXPERIMENTAL

The starting powder materials used in this study were: α-Si_3N_4 (UBE, SN-E10), TiN (H.C. Starck), Al_2O_3 (99.9% purity, Almatis CT 3000SG) and Y_2O_3 (99.99% purity, Sigma Aldrich). In order to prepare the compositions, the powders were ground in a ball mill for 24 h and dried in a rotoevaporator at 90 ºC. After drying, pellets were obtained from each composition by means of uniaxial (50 MPa) and cold isostatic (200 MPa) pressing. The sintering process was performed using a graphite resistance furnace (Thermal Technol.) under 15 psi of nitrogen gas at 1750 ºC/1 h or 1815 ºC/1 h, with a heating rate of 10 ºC/min. Table I shows the formulations of the compositions, as well as the sintering conditions.

Table I - Compositions and sintering conditions used.

Composition	Sintering conditions	Si_3N_4 (wt%)	TiN (wt%)
NSNT-1	1750 ºC/1 h	85.0	5.0
NSNT-2		80.0	10.0
NSNT-3		70.0	20.0
NSNT-4		60.0	30.0
NSNT-5	1815 ºC/1 h	85.0	5.0
NSNT-6		80.0	10.0
NSNT-7		70.0	20.0
NSNT-8		60.0	30.0

Note: in all compositions 5.0 wt% Al_2O_3 and 5.0 wt% Y_2O_3 were added.

The sintered samples were evaluated in regard to weight loss as well as the apparent density and porosity by the Archimedes method. The relative density was determined using the theoretical density (TD) of the compositions, calculated from the rule of mixtures. The crystalline phases in the sintered samples were identified by X-ray powder diffraction (XRPD) using a Bruker D8 X-ray diffractometer with CuKα radiation. The phase distribution, as well as the grain size and their morphology, was analyzed by scanning electron microscopy (SEM, Philips, XL-30) on polished samples, previously coated with a thin layer of carbon. In addition, energy dispersive X-ray spectroscopy was used to identify the chemical elements present in each phase of the composites. In order to determine the Vickers hardness (H_V, Eq. A) of the composites, the Vickers indentation method (ASTM C1327) was performed using a durometer (Buehler, VMT-7) with a pyramidal penetrator and 100 N load.

$$H_v = \frac{1.8554.P}{a^2} \quad (A)$$

where P is the applied load (N) and a corresponds to the average length of the two diagonals of the indentation (m). The fracture toughness, expressed by the critical stress intensity factor (K_{IC}) in $MPa.m^{1/2}$ (Eq. B), was obtained by means of the lengths of the impression diagonals and surface cracks measured immediately after indentations, using the equation proposed in [23]:

$$K_{IC} = 0.016\left(\frac{E}{H_V}\right)^{1/2}\frac{P}{c^{3/2}} \quad (B)$$

where H_v is the Vickers hardness (GPa), P is the applied force (N), c is the half-length of radial crack, and E is Young's modulus (GPa). The Young's modulus of the composites was computed by the rule of mixtures using the values of each individual component [7, 24, 25].

RESULTS AND DISCUSSION

Table II shows the results of relative density, apparent porosity and weight loss of the samples sintered at 1750 °C/1 h and 1815 °C/1 h. It was possible to note that the samples reached high relative densities and low apparent porosity, confirming that the selected compositions and sintering conditions were efficient in obtaining dense silicon nitride-based composites. The values of relative density obtained in the studied samples were similar to the values obtained in other studies [26, 27] where the samples were submitted to conventional sintering and also other complex sintering methods [2, 15, 21]. The samples sintered at 1750 ºC for 1 h showed relative densities slightly higher than the samples sintered at 1815 ºC for 1 h. This result can be justified by the greater weight loss and porosity found for samples sintered at 1815 ºC, probably because of the decomposition of Si_3N_4 which is more favorable at the higher sintering temperature. The lower relative density as a consequence of the increase in the sintering temperature was in agreement with a study performed by other authors [26], that analyzed the densification of a Si_3N_4-TiN composite with 30 wt% of TiN second phase and 10% of La_2O_3+AlN as sintering aids. In this study, the highest densification obtained at 1760 °C was attributed to the eutectic reaction among Si_3N_4 and the sintering aids. According to [26], below 1760 °C the amount of liquid phase increased which favored the liquid

sintering process and, consequently, the relative density of the material. Above 1760 ºC, Si_3N_4 tends to decompose and the liquid phase to vaporize, resulting in reduced values of density. Moreover, it is possible to observe in Table II that the relative density of samples presented a tendency to decrease as the TiN amount increased. This behavior was noted in the samples obtained by both sintering conditions. Perhaps, for higher contents of TiN, higher sintering temperature should be used due to its elevated thermal decomposition temperature (2930 ºC) [24, 27].

Table II - Relative density, apparent porosity and weight loss of studied samples.

Sample	Relative density (%)	Apparent porosity (%)	Weight loss (%)
NSNT-1	98.04±0.16	0.16±0.08	1.83±0.17
NSNT-2	97.95±0.13	0.20±0.06	1.79±0.19
NSNT-3	97.40±0.17	0.27±0.07	1.74±0.22
NSNT-4	97.26±0.22	0.30±0.10	1.80±0.31
NSNT-5	97.75±0.33	0.31±0.12	3.33±0.44
NSNT-6	97.62±0.13	0.31±0.07	3.20±0.55
NSNT-7	97.51±0.25	0.37±0.09	2.98±0.44
NSNT-8	96.95±0.19	0.31±0.11	3.15±0.10

The X-ray diffractograms of the sintered samples are shown in Fig. 1. For all sintering conditions, only peaks of β-Si_3N_4 and TiN were identified, demonstrating that the α-Si_3N_4 phase was totally transformed to β-Si_3N_4, independent of the initial amount of TiN in the composition. The exclusive presence of Si_3N_4 and TiN was another strong evidence of the efficiency of both used sintering parameters and selected compositions. As well, the absence of crystalline phase formed by cations of the additive oxides indicated that they were present in the grain boundaries of the material as a secondary glassy phase.

SEM micrographs of the sintered and polished sample surfaces (Fig. 2) show larger grains of TiN (white phase)

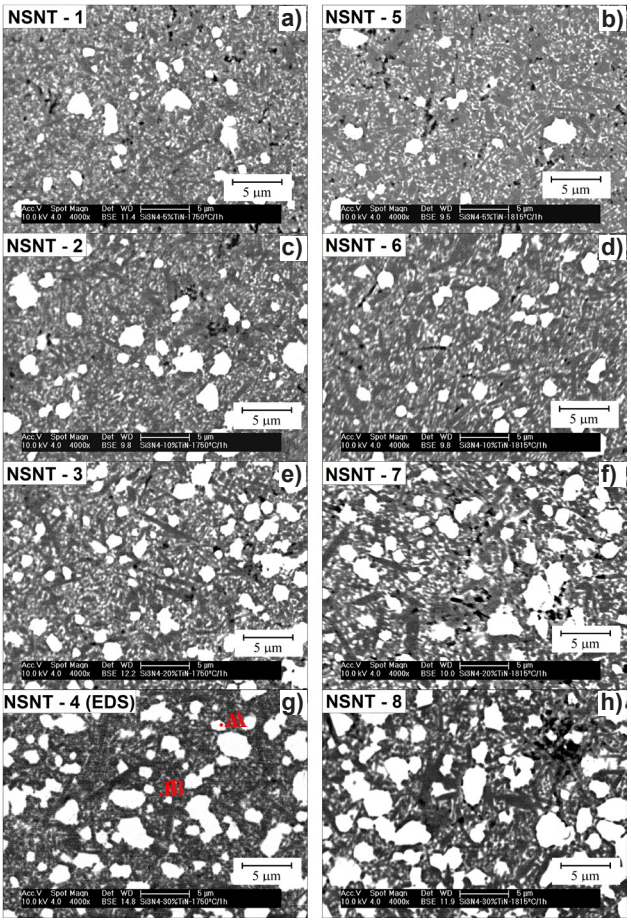

Figure 2: SEM micrographs (backscattered electron images) of the samples sintered at 1750 ºC and 1815 ºC for 1 h.

homogeneously dispersed along the β-Si_3N_4 grains (dark gray phase) and the glassy phase (light gray phase) in all studied conditions. Fig. 3 shows two EDS spectra obtained from the A and B points in the NSNT-4 sample micrograph (Fig. 2). The spectra confirmed that the dark gray phase was composed predominantly of Si, i.e. Si_3N_4, and the white phase was composed predominantly by Ti and N, i.e., TiN, as also noted in the X-ray diffractograms (Fig. 1). By the micrographs, it was also clear that the amount of TiN

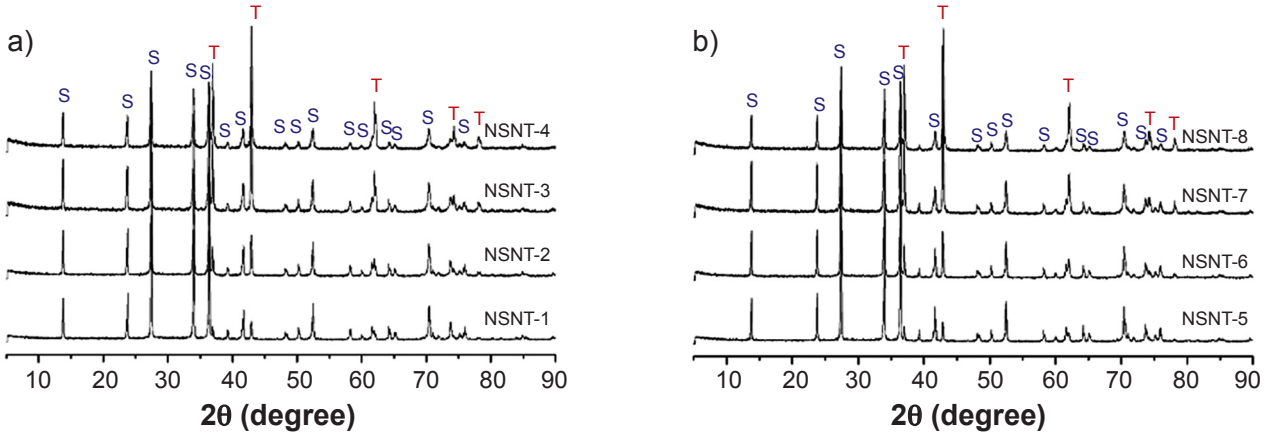

Figure 1: XRPD patterns of sintered samples at: a) 1750 ºC/1 h; and b) 1815 ºC/1 h. S is β-Si_3N_4 (PDF 33-1160) and T is TiN (PDF 87-0628).

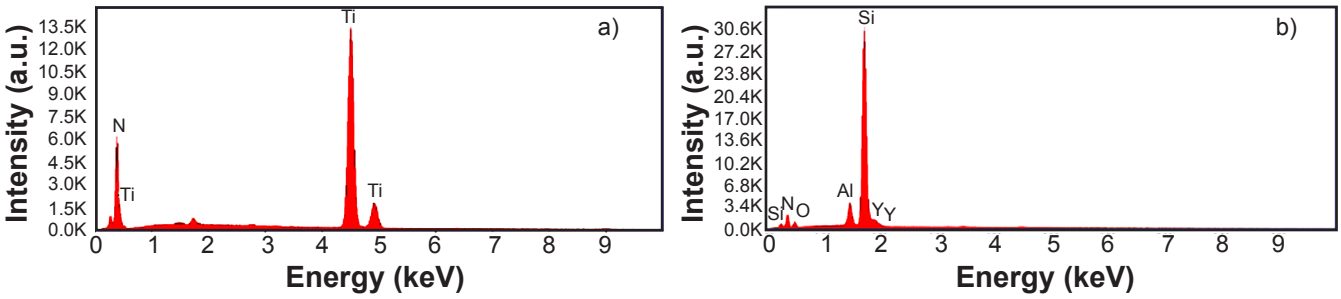

Figure 3: EDS spectra of the points A (a) and B (b) indicated in the micrograph of sample NSNT-4 containing 30% TiN sintered at 1750 ºC/1 h (Fig. 2).

Table III - Hardness and fracture toughness of studied samples.

Sample	Hardness (GPa)	K_{IC} (MPa.m$^{1/2}$)
NSNT-1	12.82±0.23	7.53±0.85
NSNT-2	13.15±0.50	8.20±0.56
NSNT-3	13.01±0.50	7.79±0.33
NSNT-4	12.77±0.46	8.95±0.58
NSNT-5	12.82±0.32	6.31±0.61
NSNT-6	12.71±0.48	7.33±0.45
NSNT-7	12.51±0.61	8.08±0.47
NSNT-8	12.53±0.21	9.27±0.72

grains increased proportionally with the increase of TiN added in the initial composition. Moreover, the elongated shape of the β-Si_3N_4 grains was also possible to verify in the micrographs. This kind of grain morphology, together with the presence of TiN phase in the material's microstructure, contributes significantly to form ceramics components with increased values of fracture toughness due to the different toughening mechanisms (crack bridging, crack deflection and microcracking) [28].

Table III shows the values of hardness and fracture toughness of the sintered samples. It was noted that the different contents of TiN did not lead to significant differences among the hardness values of the composites. On the other hand, it was possible to note that the fracture toughness reached a value of 9.27 MPa.m$^{1/2}$ for NSNT-8 sample, higher than values reported for samples obtained by different sintering processes [14, 16, 21, 26, 28]. In addition, mainly analyzing the results of the samples sintered at 1815 °C for 1 h, it was noted a tendency to fracture toughness increase with higher amounts of TiN in the compositions, as also verified in other studies [2, 26, 28].

CONCLUSIONS

The sintering conditions and the selected compositions promoted the obtention of Si_3N_4-TiN composites with high relative density and low porosity in combination with a microstructure formed by elongated grains of β-Si_3N_4 and TiN dispersed in a glassy phase. However, the samples sintered at 1750 ºC for 1 h showed better densification results, compared to those sintered at 1815 ºC for 1 h, in which the largest weight loss occurred due to Si_3N_4 decomposition. The microstructure of all composites favored the increase of fracture toughness due to the TiN grains surrounding the β-Si_3N_4 grains, while their hardness values were similar. Hence, the results suggested that the obtained composites have a potential for structural applications, although those one containing higher amounts of TiN were more promising since they tended to favor different toughening mechanisms and produce components with better fracture toughness.

ACKNOWLEDGMENT

To FAPESP, Fundação de Amparo à Pesquisa do Estado de São Paulo (Process 2015/02265-7).

REFERENCES

[1] F.L. Riley, J. Am. Ceram. Soc. **83**, 2 (2000) 245.
[2] M. Zhou, J. Zhong, J. Zhao, D. Rodrigo, Y. Cheng, Mater. Res. Bull. **48** (2013) 1927.
[3] A. Neumann, T. Reske, M. Held, K. Jahnke, J. Mater. Sci. Mater. Med. **15** (2004) 1135.
[4] A.R. Arellano-López, M.A. Mcmann, J.P. Singh, J. Martinez-Fernandez, J. Mater. Sci. **33** (1998) 5803.
[5] C. Greskovich, G.E. Gazza, J. Mater. Sci. Lett. **4** (1985) 195.
[6] H.J. Choi, K.W. Kim, J.G. Lee, J. Mater. Sci. Lett. **15** (1996) 375.
[7] P. Greil, Mater. Sci. Eng. A **109** (1989) 27.
[8] F. Monteverde, A. Bellosi, J. Eur. Ceram. Soc. **18** (1998) 2313.
[9] J. Zeng, I. Tanaka, Y. Miyamoto, O. Yamada, K. Niihara, J. Am. Ceram. Soc. **75**, 1 (1992) 148.
[10] K. Negita, J. Mater. Sci. Lett. **4** (1985) 755.
[11] Y.G. Gogotsi, J. Mater. Sci. **29** (1994) 2541.
[12] J.-F. Yang, T. Ohji, T. Sekino, C.-L. Li, K. Niihara, J. Eur. Ceram. Soc. **21** (2001) 2179.
[13] J.-F. Yang, T. Sekino, Y.-H. Cho, K. Niihara, T. Ohji, J. Am. Ceram. Soc. **84**, 2 (2001) 406.
[14] L. Gao, J. Li, T. Kusunose, K. Niihara, J. Eur. Ceram.

Soc. **24** (2004) 381.
[15] S. Zheng, L. Gao, H. Watanabe, J. Tatami, T. Wakihara, K. Komeya, T. Meguro, Ceram. Int. **33** (2007) 355.
[16] C.-C. Liu, J.-L. Huang, Ceram. Int. **29** (2003) 679.
[17] A.A. Sivkov, D.Y. Gerasimov, A.A. Evdokimov, Mater. Sci. Eng. **93** (2015) 1.
[18] H.V. Shanmugakumar, N. Veerappan, C. Ramanathan, Proc. Appl. Ceram. **10**, 3 (2016) 153.
[19] A.A. Evdokimov, A.A. Sivkov, D.Y. Gerasimov, Glass Ceram. **72**, 9-10 (2016) 381.
[20] L.A. Kondratieva, I.A. Kerson, A.Y. Illarionov, A.P. Amosov, G.V. Bichurov, Mater. Sci. Eng. **156** (2016) 1.
[21] L.A. Díaz, W. Solís, P. Peretyagin, A. Fernández, M. Morales, C. Pecharromán, J.S. Moya, R. Torrecillas, J. Nanomater. **2016** (2016) 1.
[22] F. Mussano, T. Genova, P. Rivolo, P. Mandracci, L. Munaron, M.G. Faga, S. Carossa, J. Mater. Sci. **52** (2017) 467.
[23] G.R. Antis, P. Chantikul, B.R. Lawn, D.B. Marshall, J. Am. Ceram. Soc. **64**, 9 (1981) 533.
[24] J. Russias, S. Cardinal, J. Fontaine, G. Fantozzi, C. Esnouf, K. Bienvenu, Int. J. Refract. Metals Hard Mater. **23** (2005) 344.
[25] D. Casellas, I. Ràfols, L. Llanes, M. Anglada, Int. J. Refract. Metals Hard Mater. **17** (1999) 11.
[26] W.U. Laner, J. Yong, Key Eng. Mater. **512-515** (2012) 878.
[27] I. Seki, S. Yamaura, Mater. Trans. **58**, 3 (2017) 361.
[28] A. Bellosi, S. Guicciardi, A. Tampieri, J. Eur. Ceram. Soc. **9** (1992) 83.
(Rec. 31/08/2018, Rev. 16/11/2018, Ac. 22/11/2018)